European Review for Medical and Pharmacological Sciences 2021; 25: 4693-4701

Towards real-time diagnosis for pediatric sepsis using graph neural network and ensemble methods

X. CHEN[1,2], R. ZHANG[1,2], X.-Y. TANG[1,2]

[1]University of Chinese Academy of Sciences, Beijing, China
[2]Shanghai Institute of Technical Physics of the Chinese Academy of Sciences, Key Laboratory of Infrared Detection and Imaging Technology, Shanghai, China

Abstract. – OBJECTIVE: The rapid onset of pediatric sepsis and the short optimal time for resuscitation pose a severe threat to children's health in the ICU. Timely diagnosis and intervention are essential to curing sepsis, but there is a lack of research on the prediction of sepsis at shorter time intervals. This study proposes a predictive model towards real-time diagnosis of sepsis to help reduce the time to first antibiotic treatment.

PATIENTS AND METHODS: The dataset used in this paper was obtained from the pediatric intensive care unit of Shanghai Children's Medical Center and consisted of the initial examination records of patients admitted to the hospital. The data included six groups of laboratory tests: medical history, physical examination, blood gas analysis, routine blood tests, serological tests, and coagulation tests. We divided the admission examination into three stages and proposed a sepsis prediction model towards real-time diagnosis based on local information to shorten waiting time for treatment. The model extracts homogeneous features from patient groups in real-time using a graph neural network and uses the deep forest to learn from homogeneous features and laboratory data to give a comprehensive prediction at the current stage. Discriminative features of each stage are used as augmented information for the next phase, finally achieving self-optimization of global judgment, assisting in pre-allocation of medical resources and providing timely medical assistance to sepsis patients.

RESULTS: Based on the first stage, second stage, and full test, the AUCs of our model were 93.63%, 96.73%, and 97.58%, respectively, and the F1-scores were 77.35%, 85.71%, and 86.48%, respectively. The models gave relatively accurate predictions at each stage.

CONCLUSIONS: The prediction model toward a real-time diagnosis of sepsis shows more accurate predictions at each stage compared to other control methods. When the first two stages of data are obtained as input, the model accuracy is close to using complete test data, which can help compress the time to diagnosis to about an hour after the test and significantly reduce waiting time.

Key Words:
Pediatric sepsis, Real-time diagnosis, Graph neural network, Tree-based model, Ensemble method.

Introduction

Sepsis is a common complication of infection in the pediatric intensive care unit (PICU) and is also a leading cause of death[1]. Studies have shown that the optimal resuscitation time for patients with sepsis is within 6 hours of the onset of the disease. Mortality may further increase if patients with severe sepsis are not promptly treated with antibiotics. The mortality rate increases by 6% for each one-hour delay in receiving antibiotic therapy after the onset of septic shock hypotension[2]. The real-time prediction of pediatric sepsis is thus crucial to improving survival rates.

With the development of electronic health records (EHR) and artificial intelligence, researchers have proposed methods that can provide accurate prediction of sepsis at an early stage. Zhang et al[3] used Lasso to construct a sepsis prediction model, while Wang et al[4] proposed a kernel extreme learning machine (KELM) to predict disease probabilities. Masino et al[5] used the AdaBoost algorithm to predict patient data and found that the performance of machine learning was not inferior to bacterial culture detection in prediction. Le et al[6] used gradient-enhanced decision trees (GBDT) to provide early warning of sepsis in children. Recurrent neural network-based

Corresponding Author: Xiao Chen, MD; e-mail: nalanyu2000@163.com

approaches have also been proposed to process clinical data for sepsis with a temporal structure (e.g., heart rate, respiration, blood pressure, and blood oxygen). Futoma et al[7] proposed Gaussian process recurrent neural networks to model physiological data, while Fagerström et al[8] proposed a LiSep long short-term memory (LSTM) model for early sepsis detection. Bedoya et al[9] developed the MGP-RNN model to verify that deep learning models can detect sepsis earlier and more accurately than baseline methods. Although some of the above methods use the patient's first admission examination records to predict sepsis, the lengthy complete examination can delay the treatment of critically ill patients.

Patients are usually given a thorough examination upon admission to the ICU. The initial ICU admission examination usually consists of six tests: anamnesis, physical examination, blood gas analysis, blood routine examination, serology, and coagulation tests. It takes 3-4 hours to obtain the results for all of these tests. If the diagnosis is not made until all of the test results are available, the best opportunity for the patient's treatment may be missed.

In this paper, we propose a sepsis prediction model towards a real-time diagnosis that may predict sepsis infection based on partial laboratory data. The model aims to help shorten the time to first antibiotic treatment and to avoid failure to provide life-saving treatment to patients due to waiting for time-consuming lab results. We divide each test into three different groups according to the time to get results. The first stage includes anamnesis, physical examination, and blood gas analysis, which allows for immediate results. The second stage comprises routine blood examination, such as routine blood and reactive proteins, which can be obtained within half an hour to one hour. The last stage includes serological and coagulation tests, the results of which take at least 3-4 hours to obtain.

The main contributions of this paper can be summarized as follows: (1) We propose a BalanceEnsemble hybrid integration model that outperforms comparable baseline methods; (2) we propose a multi-activations autoregressive moving average (MA-ARMA) graph neural network for patient homogeneity feature learning extraction; and (3) we propose a phased sepsis prediction model oriented toward real-time prediction. The proposed model can output accurate sepsis prediction at an early stage, shorten the time required for initial diagnosis, and enable sepsis patients to receive antibiotic treatment earlier. The prediction results gradually improve with gradual data refinement.

Patients and Methods

Study Population

The dataset for this paper was collected from the PICU at Shanghai Children's Medical Center; it contains the clinical records from 2010 to 2017 of the patients' first examination after admission and the diagnostic results.

General diagnosis criteria for sepsis include Sequential Organ Failure Assessment score (SOFA) and Quick Sequential Organ Failure Assessment (qSOFA). In clinical diagnosis, organ dysfunction can be indicated by a SOFA with an increase of more than or equal to 2 points. The higher the SOFA score gets, the more severe the patient's condition is. Some indicators of the SOFA scores require blood test results, which poses a barrier to the employment of SOFA for patient's assessment in clinical practice. Regarding the practicality, experts have selected three clinically available indicators to construct a quick and simplified version of the SOFA, called qSOFA[10]. qSOFA scores include altered mental status, systolic blood pressure less than or equal to 100 mmHg, and respiratory frequency less than 22 breaths/min. qSOFA allows for rapid screening of septic patients outside the ICU.

Considering that this is a retrospective study, the final diagnosis of sepsis patients was determined by clinicians from a combination of qSOFA, SOFA, and bacilli culture results.

The inclusion criteria for patients in the dataset were (a) age <18 years and (b) a PICU stay greater than or equal to 2 days. The exclusion criteria were (a) proportion of missing values in data <60% and (b) incomplete electronic medical records due to abandoned treatment or transfer.

After removing a large sample of missing values, the dataset included a total of 3,298 patients, including 445 cases of sepsis. Based on clinical experience and previous literature, the clinical laboratory categories selected for this paper included medical history, physical examination, blood gas analysis, routine blood, serological tests, and coagulation tests.

According to clinical experience and the existing literature, we chose six kinds of indexes—anamnesis, physical examination, blood gas, routine blood examination, serum, and coagulation

Table I. Characteristics of PICU patients.

Characteristics		Total		Sepsis	
		Count	(%)	Count	(%)
Gender	Male	1282	38.8	274	61.6
	Female	2015	61.2	171	38.3
Age	0-1	1264	38.3	162	36.4
	2-5	1197	36.3	146	32.2
	6-12	589	17.9	89	20
	13-17	247	7.5	48	10.7

tests—to construct the model. The selection of these tests is based on diagnostic criteria such as SOFA, qSOFA and practical clinical experience. The physical examination contains the items required for the qSOFA score and is even more comprehensive. Laboratory tests such as routine blood examination, serum, and coagulation have more comprehensive indicators than those involved in SOFA and can provide more valid information for the prediction

According to their consuming time, the six group examinations are divided into three stages. The first stage comprises medical history, physical examination, blood gas analysis, such as fever history, tumor, poor spirits, cyanosis of the lip, cyanosis, tri-retraction sign, pulmonary rales, temperature, heart rate, respiratory rate, SPO2, blood pressure, Lac, PaCO2, PaO2, O2SAT, PH, FreeCa, K+, Na+, CL-, HCO3-, capillary refill time (CRT). The second stage includes routine blood examination, such as white cell count, hemoglobin determination, hematocrit determination, platelet count, neutrophil number, neutrophil ratio, monocyte number, lymphocytes number, Lymphocyte ratio, C-reactive protein. The third stage contains serum, and coagulation test, including creatinine (CREA), Total Protein (TP), total bilirubin (TBIL), albumin (ALB), aspartate aminotransferase (AST), UREA, Gamma-glutamyl transferase (GGT), unconjugated bilirubin (UNCONJ.BILI), conjugated bilirubin (CONJ.BILI), prothrombin time (PT), Activated Partial Thromboplastin Time (APTT), fibrinogen (FIB), D-Dimer (D-D), thrombin time (TT), international normalized ratio (INR).

Predictive Models Towards Real-Time Diagnosis

In this paper, we propose a three-stage cascade model for real-time sepsis diagnosis that outputs predictions based on partial data at each stage. The corresponding module for each stage has essentially the same structure and consists of a graph neural network and tree-based model. The details of the model are shown in Figure 1. The inputs for stage 1 include anamnesis, physical examination, and blood gas analysis. We also modeled the patients and their medical records as a graph network. In a graph network structure, neighbor nodes with similar features usually have the same label, which means that the neighbors of sepsis patients are also likely to be sepsis patients. It is well known that similar people share similar characteristics; this is known as homogeneity. We therefore apply the proposed MA-ARMA graph convolutional network (GCN) to extract homogeneous features for each data stage, and the deep forest is used to learn high-dimensional discriminative features for the learned isomorphic features and input data, making it possible to provide predictions for the current stage. The discriminative features learned by each stage module are propagated to the next stage as augmented information for further learning and providing discriminative information for prediction. That is, the modules in different stages are cascaded through the discriminative features propagated from the previous stage. The input of the second stage is the fusion vector of the routine blood examination and the discriminative features learned from the first stage. The final-stage input fuses the second-stage discriminative features with serological examination and coagulation tests. The model structure of the latter two stages is also identical to that of the first stage.

MA-ARMA Graph Convolutional Neural Network

Patients in the PICU can be divided into sepsis and non-sepsis groups, and in this study, patient clinical data are considered as graph data with a bipartite structure. Each patient constitutes a node in the graph network, and the patient's

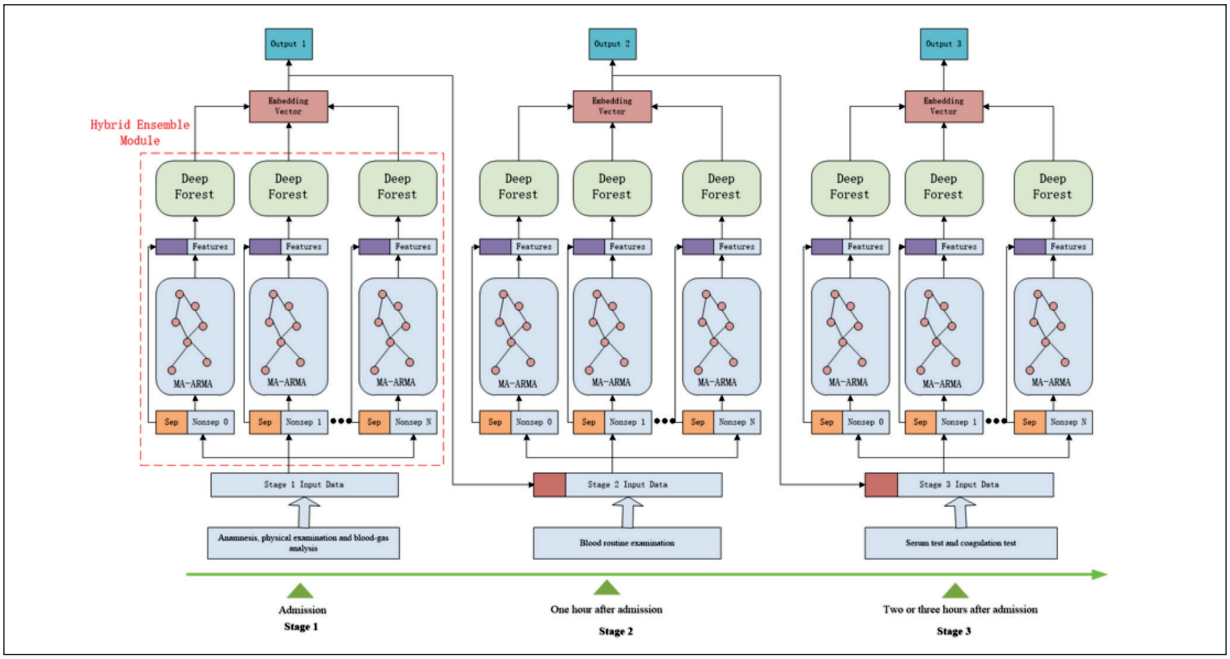

Figure 1. Schematic diagram of model structure: three identical cascade modules that make predictions based on the assay results of the corresponding stage.

clinical records are used as attributes of the node. We computed the neighbor nodes for each patient node using the k-nearest neighbor algorithm, where k=5. We connected each patient with the five most similar patients. The homogeneous features can illuminate information beyond the individual patient for classification.

We propose an MA-ARMA GCN to extract homogeneous features among patients. The MA-ARMA GCN is a multi-activation function convolution network based on the ARMA filter. Compared with commonly used polynomial filters, ARMA filters can fit more complex signal responses and are more robust, thus reducing the dependence on the graph structure. An MA-ARMA network provides different activation functions for each layer of neurons, thus generating different distributions of response signals. The diverse response signals increase the flexibility and diversity of the neural network, which can effectively suppress the over smoothing problem and improve the generalization ability of the model.

The MA-ARMA network consists of ARMA convolutional layers (ARMA-Conv) and multi-activations layers (MA). The ARMA-Conv is a graph convolution layer composed of ARMA graph filters[11]; it can simulate more filters with better spectral processing capabilities. The MA layer allows neurons to choose different activation functions to obtain different high-dimensional mapping vectors. The structure of the MA-ARMA GCN is shown in Figure 2.

ARMA Convolutional Layers

GCNs based on autoregressive moving average (ARMA) filters have greater robustness and can approximate a variety of different filter shapes to provide more graph frequency responses. The expression of the K-order ARMA filter is[11],

$$h_{\mathrm{ARMA_K}} = \frac{\sum_{k=0}^{K} p_k \lambda_k}{1 + \sum_{k=1}^{K} q_k \lambda_k} \tag{1}$$

where L is the standard Laplacian matrix of the graph, λ is the eigenvalue of L.

The output signal of the ARMA convolution can be written as

$$\bar{X} = (1 - \sum_{k=0}^{K} q_k L^k)^{-1} (\sum_{k=0}^{K-1} p_k L^k) X \tag{2}$$

where X is the initial node feature.

MA-ARMA Convolution Layer

Traditional neural networks use uniform activation functions for each layer, such as all relu or leaky relu, so each network layer can only fit a sin-

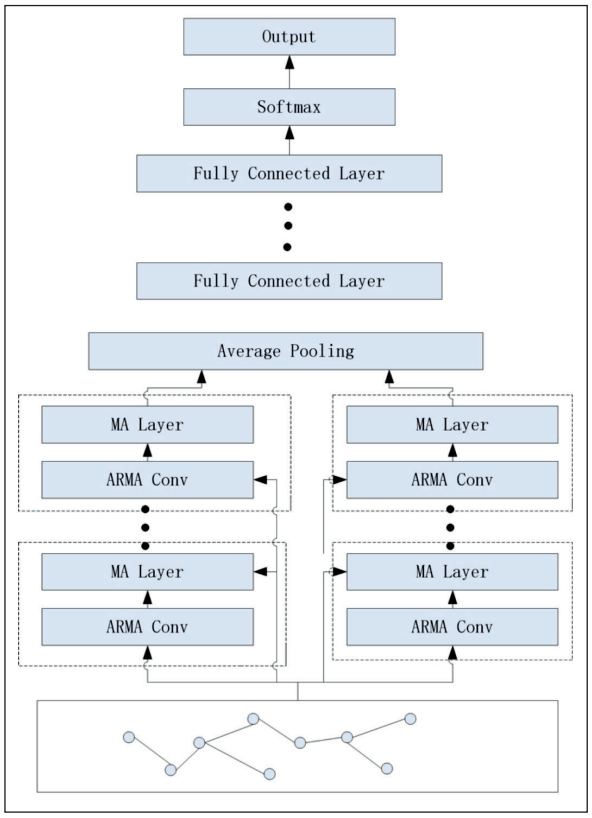

Figure 2. Schematic diagram of the MA-ARMA GCN.

gle data distribution. We proposed an MA-ARMA GCN in which each activation layer in the network consists of different kernel activation functions, and neurons can correspond to different activation functions. MAs can increase the flexibility and diversity of a neural network and to a certain extent can alleviate the problem of over smoothing in GCNs[12]. The MA function is defined as follows:

$$MA(s) = \sum_{i=1}^{D} \alpha_i \, k(s, d_i) \tag{3}$$

$$k(s, d_i) = exp\{-\gamma(s - d_i)^2\} \tag{4}$$

where D is a hyperparameter indicating the total number of different kernel activation functions in the current MA layer; denotes the adaptive weighting coefficients; is a linear expression, which can be interpreted as wxi+b (we use the letter to represent the single input of the function); $k(\ldots)$ denotes the one-dimensional Gaussian kernel; and denotes the dictionary element. The dictionary of the kernel function is determined by even steps of x with mean 0. $\gamma \in R$ denotes the bandwidth of the kernel. The kernel functions map low-dimensional data to a high-dimensional space. The different kernel functions represent a diversity of varying data mappings and high-dimensional projections, and the increased diversity also means a greater possibility of finding hyperplanes to partition the data. A mathematical expression for the output $\bar{X}^{(t+1)}$ of the (t+1)-th ARMA-Conv layer with a multivariate activation function is as follows:

$$\bar{X}^{(t+1)} = \sum_{i=1}^{D} \alpha_i \, k\left(\tilde{L}\bar{X}^{(t)}W^{(t)} + XV^{(t)}, d_i\right) \tag{5}$$

Hybrid Ensemble Model Based on BalanceEnsemble Method

There is a severe category imbalance problem in the dataset, which would lead to poor performance if used directly as input to the GCNs. We therefore proposed a BalanceEnsemble method and constructed a hybrid ensemble model (HEM) with it. The minority class sample is the sample of septic patients, also called the positive sample. The core idea of the BalanceEnsemble is to retain all positive samples and match different negative samples to form a new training set for the model. The process of BalanceEnsemble is as follows:

1. Select all positive sample data.
2. Randomly select a group of negative samples whose total number is equal to the positive samples and repeat the operation n times to get n groups of negative samples.
3. Combine all of the positive samples and different groups of negative samples to obtain n different training sets.
4. Train the model with n training sets and weigh the results to obtain the final results.

We built the HEM based on the BalanceEnsemble strategy, which consists of several parallel feature-decision branches, each of consists of two modules in series: a feature extractor and a decision classifier. The feature extractor is an MA-ARMA network, which extracts patients' homogeneous features. The decision classifier is a deep forest, which predicts patients based on the input information. The HEM acts as an information-processing module at each stage, accepting the corresponding clinical data information and yielding the prediction. The embedding vectors learned in each stage of the HEM are used as augmentation features to be fused into the input of the next stage. The specific structure of the HEM is shown in Figure 3.

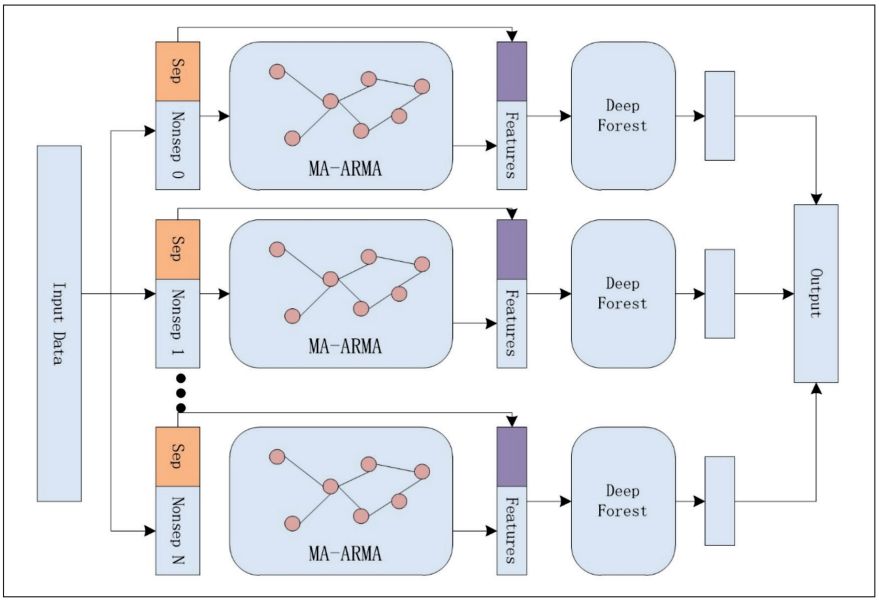

Figure 3. Schematic diagram of the hybrid ensemble model framework.

We used the random forest, gradient boosting decision tree (GBDT), support vector machine (SVM), residual neural network (ResNet), LSTM, and GCN as the baseline models for the experiment. The experimental data were divided into a training set and a test set. The data from 2010 to 2016 were used as the training set. K-fold cross-validation (K=4) was used to verify algorithm performance. The data from 2017 were used as the test set to evaluate model performance. The results are shown in Table II, Table III, and Table IV. The AUCs are shown in Figure 4.

Table II. Performance results for each model at stage 1.

Name	ACC	AUC	F1	Sensitivity	Specificity
GCN[13]	0.8046	0.7595	0.3707	0.3704	0.8843
LSTM[14]	0.8103	0.8475	0.5285	0.6851	0.8333
Logistic[15]	0.8506	0.8850	0.5928	0.7037	0.8776
ResNet[16]	0.8506	0.8644	0.5937	0.7037	0.8775
MLP[17]	0.8591	0.8413	0.5950	0.667	0.8945
SVM[18]	0.8621	0.8838	0.6190	0.7222	0.8878
RF[19]	0.8908	0.9235	0.6935	**0.7963**	0.9081
GBDT[20]	0.9023	0.9289	0.7119	0.7778	0.9251
DF[21]	0.9281	0.9227	0.7524	0.7037	**0.9693**
Ours	**0.9331**	**0.9363**	**0.7735**	0.7592	0.9626

Table III. Performance results for each model at stage 2.

Name	ACC	AUC	F1	Sensitivity	Specificity
GCN[13]	0.8218	0.7504	0.4364	0.4444	0.8911
LSTM[14]	0.8390	0.8799	0.5942	0.7592	0.8537
ResNet[16]	0.8621	0.9196	0.6307	0.7592	0.8809
MLP[17]	0.8793	0.8852	0.6315	0.6667	0.9183
Logistic[15]	0.8707	0.9363	0.6512	0.7778	0.8878
SVM[18]	0.8879	0.9498	0.6609	0.8518	0.8911
RF[19]	0.9080	0.9457	0.7333	0.8148	0.9251
GBDT[20]	0.9367	0.9527	0.78	**0.8722**	**0.9761**
DF[21]	0.9396	0.9567	0.8037	0.7963	0.9659
Ours	**0.9568**	**0.9673**	**0.8571**	0.8333	0.9759

Table IV. Performance results for each model at stage 3.

Name	ACC	AUC	F1	Sensitivity	Specificity
GCN[13]	0.7816	0.8167	0.4412	0.5556	0.8231
LSTM[14]	0.8793	0.9132	0.6250	0.6481	0.9217
ResNet[16]	0.8793	0.9110	0.6557	0.7407	0.9047
MLP[17]	0.8851	0.9124	0.6875	0.8148	0.8979
SVM[18]	0.8851	0.9505	0.7015	0.8703	0.8877
Logistic[15]	0.8965	0.9566	0.7049	0.7962	0.9149
GBDT[20]	0.9109	0.9684	0.7596	**0.9074**	0.9115
RF[19]	0.9195	0.9698	0.7704	0.8703	0.9285
DF[21]	0.9511	0.9639	0.8316	0.7778	**0.9829**
Ours	**0.9569**	**0.9758**	**0.8648**	0.8889	0.9693

Results

According to the performance tables for the three stages, the model proposed in this paper achieved better results than baseline on the prediction task with F1-scores of 0.7735, 0.8571, and 0.8648 for the three stages. The next best performance was that of the deep forest model, with F1-scores of 0.7524, 0.8037, and 0.8316. The convolutional neural network-based models and the recurrent neural network-based models were unable to achieve desirable performance. The

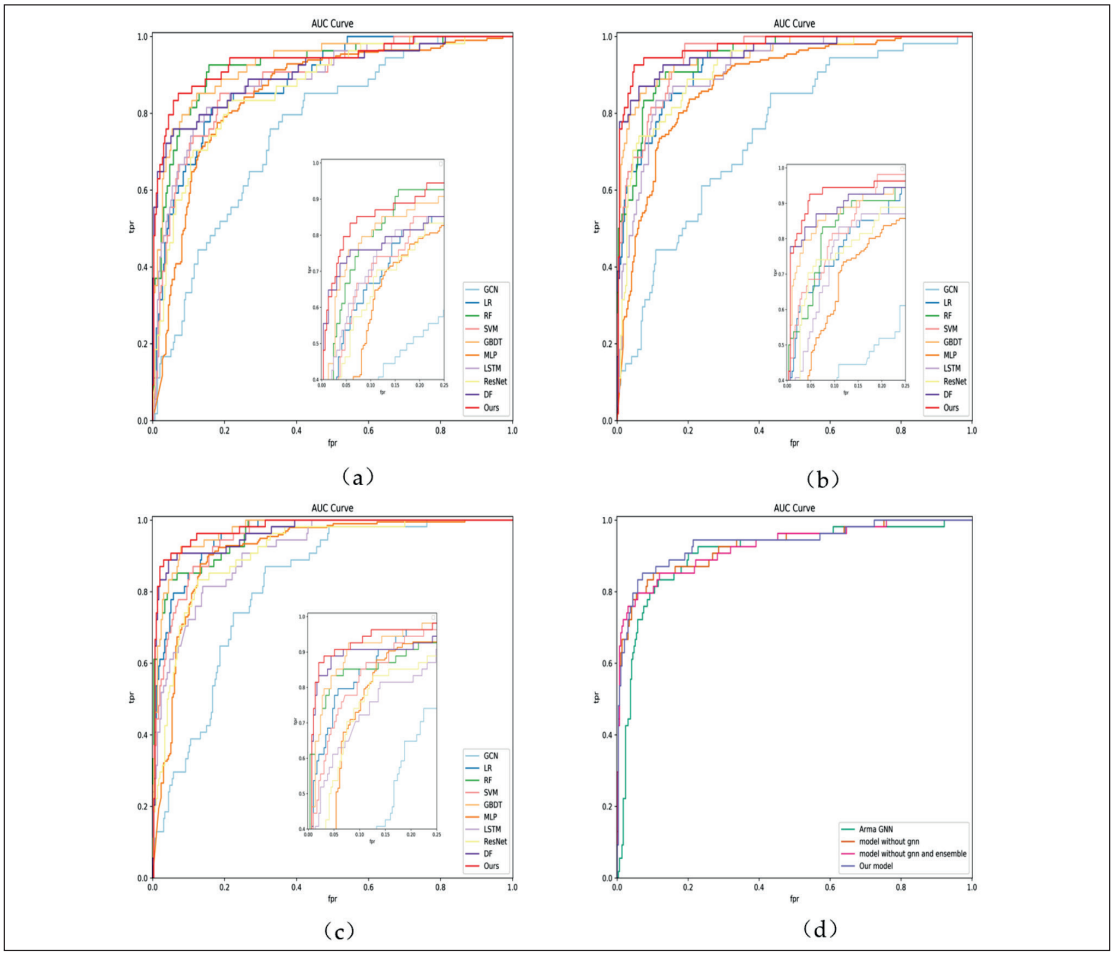

Figure 4. AUC for dataset; (**a**) AUC for phase 1; (**b**) AUC for phase 2; (**c**) AUC for stage 3; (**d**) AUC for stage 1 ablation experiment.

F1-scores for the three stages for LSTM were 0.5285, 0.5942, and 0.6250, respectively, and the F1-scores for ResNet were 0.5937, 0.6307, and 0.6557, respectively.

To verify the soundness and validity of the model structure, ablation experiments were conducted to validate the performance of the various modules. The models in the ablation experiments are referred to as the Model without GNN (MWG), Model without GNN and Ensemble Learning (MWGE), and ARMA-based GNN (AGNN). We evaluated the ablation experiments on the first-stage dataset, and the results are shown in Table V.

Discussion

Combining the performance tables for all three stages, the performance of the deep neural network was far inferior to that of the tree-based models. The main reason for this may be that the tabular clinical laboratory data lack clear spatial structures or temporal correlations. Traditional machine learning models, especially tree-based models, may be more advantageous when dealing with tabular data because they divide the high-dimensional space based on data attributes to obtain a series of subspaces. The splitting nodes in the tree-based models are highly consistent with the structure of the tabular data, which is an important reason to integrate the tree-based model into the design. As shown in Table V, the model proposed in this paper outperformed the other models, obtaining notably better results for the AUC and F1-score. Higher AUC and F1-score mean more accurate sepsis identification and lower false negatives without a significant increase in false positives.

In terms of changes in model performance at each stage, the AUC and F1-score of the first stage model are 0.9363 and 0.7735, respectively, which means that the model can immediately obtain a relatively accurate judgment based on the first-stage data alone. From stage 1 to stage 2, the model achieves a more significant performance improvement compared with the first stage, with the AUC and F1-score improving by 3.31% and 10.8%, respectively. From stage 2 to stage 3, the performance improvement of the model is smaller compared to stage 2, with the AUC and F1-score improving by 0.87% and 0.89%, respectively. The prediction from stage 2 can thus be approximated as the model's final prediction for patients. Considering that it takes only 1 hour to obtain the laboratory results for stage 2, we can thus reduce the minimum time for patients to receive antibiotic treatment to 1 hour.

The performance gradually decreased with the removal of sub-modules from the current model. From the entire model to the MWG model, sensitivity decreased from 0.77778 to 0.7407. According to the equation defining sensitivity, a decrease in sensitivity means reducing the number of correctly identified septic patients (tp) and an increase of misclassified septic patients (fn). The model became less sensitive to sepsis and tilts toward classifying all patients as routine patients. Specificity measures the ability to correctly identify regular patients (negative sample), so the negative bias of the model led to a slight rise in specificity.

The Ensemble method was good at improving generalization and avoiding over-fitting. The representation learned from the GCN also brought in different information, thus contributing to the accurate prediction of the total model from a new perspective. GNN extracted the individual patient data features and the homogeneity of the neighborhood data, thus enhancing the diversity of features and improving model performance.

Conclusions

In this paper, we proposed a real-time sepsis diagnosis prediction model to decrease the time to first antibiotic treatment for patients with sepsis. The model divides the six individual tests for sepsis diagnosis into three stages according to

Table V. Results of ablation experiments.

Name	ACC	AUC	F1	Sensitivity	Specificity
AGNN	0.8965	0.9082	0.6896	0.7407	0.9659
MWGE	**0.9281**	0.9227	0.7524	0.7037	**0.9693**
MWG	**0.9281**	0.9332	0.7619	0.7407	0.9625
Ours	0.9252	**0.9337**	**0.7636**	**0.7778**	0.9523

the time required for each test. Based on the data available at different stages, our model predicted the likelihood of sepsis in patients so that patients with high prevalence could be treated with timely intervention. We validated the performance of the model on a dataset collected from Shanghai Children's Medical Center. The results indicated that the cascaded model proposed in this paper achieved more accurate prediction in all cases compared to the baseline model. The contribution of each submodule was also demonstrated in the ablation study. Compared to previous studies, our study provides a new perspective for predicting sepsis dynamically and in real time using data from different stages, allowing patients to receive timely treatment. In the future, we hope that our approach can be extended to the predictive analysis of other similar conditions, especially those requiring timely diagnosis and therapeutic intervention.

Conflict of Interest

The Authors declare that they have no conflict of interests.

References

1) Singer M, Deutschman CS, Seymour CW, Shankar-Hari M, Annane D, Bauer M, Bellomo R, Bernard GR, Chiche JD, Coopersmith CM, Hotchkiss RS, Levy MM, Marshall JC, Martin GS, Opal SM, Rubenfeld GD, van der Poll T, Vincent JL, Angus DC. The Third International Consensus Definitions for Sepsis and Septic Shock (Sepsis-3). JAMA 2016; 315: 801-810.
2) Kumar A, Roberts D, Wood KE, Light B, Parrillo JE, Sharma S, Suppes R, Feinstein D, Zanotti S, Taiberg L, Gurka D, Kumar A, Cheang M. Duration of hypotension before initiation of effective antimicrobial therapy is the critical determinant of survival in human septic shock. Crit Care Med 2006; 34: 1589-1596.
3) Zhang Z, Hong Y. Development of a novel score for the prediction of hospital mortality in patients with severe sepsis: the use of electronic healthcare records with LASSO regression. Oncotarget 2017; 8: 49637-49645.
4) Wang XC, Wang ZY, Weng J, Wen CC, Chen HL, Wang XQ. A New Effective Machine Learning Framework for Sepsis Diagnosis. IEEE Access 2018; 6: 48300-48310.
5) Masino AJ, Harris MC, Forsyth D, Ostapenko S, Srinivasan L, Bonafide CP, Balamuth F, Schmatz M, Grundmeier RW. Machine learning models for early sepsis recognition in the neonatal intensive care unit using readily available electronic health record data. PLoS One 2019; 14: e0212665.
6) Le S, Hoffman J, Barton C, Fitzgerald JC, Allen A, Pellegrini E, Calvert J, Das R. Pediatric Severe Sepsis Prediction Using Machine Learning. Front Pediatr 2019; 7: 413-428.
7) Futoma J, Hariharan S, Heller K. Learning to Detect Sepsis with a Multitask Gaussian Process RNN Classifier 2017; 70: 1174-1182.
8) Fagerström J, Bång M, Wilhelms D, Chew MS. LiSep LSTM: A Machine Learning Algorithm for Early Detection of Septic Shock. Sci Rep 2019; 9: 15132.
9) Bedoya AD, Futoma J, Clement ME, Corey K, Brajer N, Lin A, Simons MG, Gao M, Nichols M, Balu S, Heller K, Sendak M, O'Brien C. Machine learning for early detection of sepsis: an internal and temporal validation study. JAMIA Open 2020; 3: 252-260.
10) Seymour CW, Liu VX, Iwashyna TJ, Brunkhorst FM, Rea TD, Scherag A, Rubenfeld G, Kahn JM, Shankar-Hari M, Singer M, Deutschman CS, Escobar GJ, Angus DC. Assessment of Clinical Criteria for Sepsis: For the Third International Consensus Definitions for Sepsis and Septic Shock (Sepsis-3). JAMA 2016; 315: 762-774.
11) Bianchi FM, Grattarola D, Livi L, Alippi C. Graph Neural Networks with Convolutional ARMA Filters. IEEE Trans Pattern Anal Mach Intell 2021; PP. doi: 10.1109/TPAMI.2021.3054830. Epub ahead of print. PMID: 33497331.
12) Scardapane S, Van Vaerenbergh S, Totaro S, Uncini A. Kafnets: Kernel-based non-parametric activation functions for neural networks. Neural Netw 2019; 110: 19-32.
13) Kipf T, Welling M. Semi-Supervised Classification with Graph Convolutional Networks. ArXiv 2017; abs/1609.02907.
14) Hochreiter S, Schmidhuber J. Long Short-Term Memory. Neural Computation 1997; 9: 1735-1780.
15) Cramer, J. S. The origins of logistic regression. 2002.
16) Kaiming H, Zhang XY, Ren SQ, Sun J. Deep Residual Learning for Image Recognition. Computer Vision and Pattern Recognition 2016: 770-778.
17) Rumelhart DE, Hinton GE, Williams RJ. Learning internal representations by error propagation. Parallel distributed processing: explorations in the microstructure of cognition 1988; 1: 318-362.
18) Corinna C, Vapnik V. Support-Vector Networks. Machine Learning 1995; 20: 273-297.
19) Breiman L. Random forest. Machine Learning 2001; 45: 5-32.
20) Chen TQ, Guestrin C. XGBoost: A Scalable Tree Boosting System. Knowledge Discovery and Data Mining. Proceedings of the 22nd ACM SIGKDD International Conference on Knowledge Discovery and Data Mining 2016: 785-794.
21) Zhou ZZ, Feng J. Deep Forest: Towards An Alternative to Deep Neural Networks. Proceedings of the Twenty-Sixth International Joint Conference on Artificial Intelligence 2017: 3553-3559.